Concepts for Bitrate Enhancement and Latency Reduction in Recurring Disturbed CAN FD Networks

Carina Austermann, Stephan Frei
On-board System Lab
TU Dortmund University
Dortmund, Germany
carina.austermann@tu-dortmund.de

***Abstract* — The automotive wiring harness poses a challenging electromagnetic environment with its extension and small distances between wires. The introduction of high voltage applications and Wide-Band-Gap (WBG) semiconductors in power electronic systems leads to steeper slopes of control signals, e.g. PWM signals. These signals can cause serious coupling to communication wires and reduce the bitrate. As the safety and reliability of communication are essential requirements of new technologies like autonomous driving, immunity of communication systems has to be investigated. This paper shows a theoretical analysis on the impact of recurring disturbances on communication performance caused by wire coupling. To reduce the impact of disturbance, cooperative operating strategies of the power electronic system and the communication system are proposed to avoid serious delays or bitrate reductions. The presented cooperative operating strategy is an adapted access method based on available time-triggered concepts.**

Keywords* — *EMI, time-triggered communication, PWM, CAN FD

I. Introduction

In driver assistance systems up to automated driving, the reliability of fast data transmission becomes very important. A bus system with higher data rate is CAN FD (Controller Area Network with Flexible Data rate) with up to 8 Mbit/s ([1], [2]). A further bus concept is already in development: CAN XL is proposed to reach data rates up to 10 Mbit/s and longer frames with data fields up to 2048 Byte [3]. CAN FD is a multi-master serial bus using differential signaling on an unshielded twisted wire [1]. Consequently, this system is a good example of modern bus systems, which have to meet the requirement of reliable high data rates on unshielded transmission lines. The missing shielding enables the coupling of interference signals, e.g. from switching control devices. Therefore, detailed investigations on the electromagnetic compatibility of communication systems are necessary.

In automotive power electronics, WBG semiconductors become more and more attractive. The good thermal properties in combination with operating frequencies up to the megahertz range and high operating voltages lead to an improvement in efficiency [4]. Therefore, many power electronic automotive applications are developed based on WBG semiconductors e.g. DC/DC-converters, motor drive applications, power distribution units [5]. On the other hand, the short rise times of a few nanoseconds, which ensure the high efficiency, can cause radiated emissions within a wide frequency spectrum [6] and serious coupling to wires nearby. This can induce disturbing pulses on communication wires, which can affect communication if data transmissions and switching operations take place at the same time. The problem of a partially occupied transmission channel is well known in wireless communication systems. Many different methods of adapting the transmission due to the current properties of the channel have already been discussed (e.g. [7], [8], [9]). In [7] the transmission frequency is selected to reduce the impact of jamming within a radar network. Whereas an adaptive modulation is introduced in [8] to compensate the fading properties of the channel. In this work, the idea of adapted operation of communication based on disturbances of the transmission path should be transferred to wired communication systems.

Inside of vehicles, EMC can be controlled much easier than in most other systems. The disturbing systems and the communication systems are defined together by the automotive manufacturers. With the knowledge about both, possible source of EMI and communication systems, they can control weather there is an independent operation of the systems or weather a synchronous operation shall be implemented. The general approach of the introduced cooperative operation concept is shown in Fig. 1. The superposition of disturbance and bus signal leads to faulty transmissions and high latencies. To reduce the impact of disturbing pulses, the communication takes place within times of no interference.

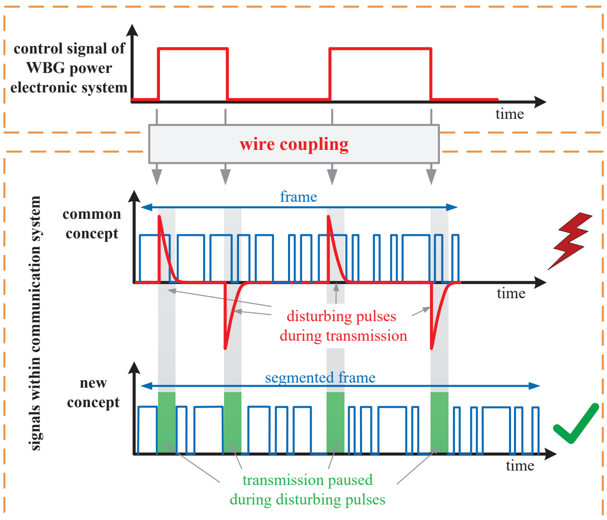

Fig. 1. Concept of adapted operation of communication based on disturbances to reduce impact on transmission

The purpose of this paper is to analyze the potential conflicts between the bus access methods and a recurring disturbance on the bus wires. In section II, the problem setting and the characteristic of the disturbing signal on the transmission lines are described. Section III analyzes different access methods and their impact on the achievable transmission rate. With the help of simulations, a configuration with a DC/AC-converter as source of the disturbing signal is analyzed in detail (section IV). In particular, bitrate reduction and latency are considered in this investigation. Finally, section V concludes this paper.

II. Electromagnetic Environment of Communication Systems

In this chapter, the electromagnetic environment and the investigated setup is introduced. The disturbing signal, which is used in the following investigations, is analyzed and described mathematically.

A. Problem setting

The proximity of power electronic systems to transmission lines lead to coupling effects, which can affect a data transmission. In [10] an electric drive system of a city bus is analyzed. The electromagnetic interactions between the systems are investigated. The problem of an interrupted communication caused by disturbing coupling effects is outlined and it was proposed to optimize the hardware design reducing the emissions. Here, a different approach is introduced to reduce the possible influence of the existing disturbance.

The coupling configuration investigated in this paper is shown in Fig. 2 and consists of simplified communication and power electronic networks. The simplified communication system consists of two CAN FD transceivers and an unshielded twisted wire pair (TWP) to build up a point-to-point connection. The characteristic termination is 120 Ω, according to ISO 11898 standard specification [2]. A split termination with two resistive loads of 60 Ω and a capacitor with 4.7 nF is used to filter and stabilize the common mode of the bus. It is assumed, that the wire of a simple power electronic system, e.g. an electromagnetic valve control, is in the proximity of the TWP. This power electronic system is built up from a resistive load and a control device, in the figure represented by a half bridge.

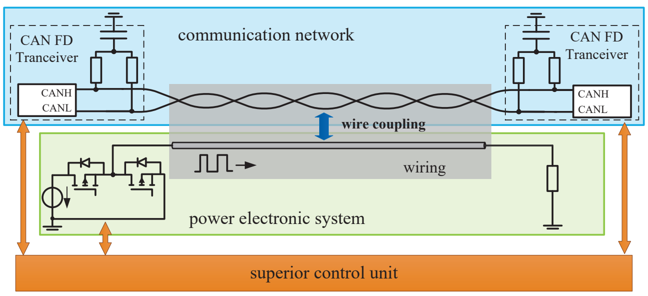

Fig. 2. Investigated setup

The control signal generated by power electronics induces especially common mode disturbances on the transmission wires, whereas differential mode disturbances could be minimized by twisting the wires. The common mode range within a transceiver can operate in normal mode is limited. E.g. the CAN FD transceiver TLE9251V [11] from Infineon operates in normal mode, according to the data sheet, only if the common mode voltage on communication wires is in the range from -12 V to +12 V. These values can be exceeded or undershot by disturbances and communication can be interrupted.

B. Characterization of interference

The switching events of the power electronic device are the source of interference. Therefore, the control signal and the coherence to the induced disturbance are described and analyzed in the following. A general control signal consists of trapezoidal pulses as shown in Fig. 3. A disturbance caused by wire coupling occurs in a case of a switching edge $t_{\mathrm{E}}(n)$. One rectangular pulse generates two disturbing pulses triggered by the rising and falling switching edges. These disturbances divide the considered time period in different time slots. The duration of disturbing pulse $t_{\mathrm{D}}(n)$ depends on geometry parameters as coupling length and distance between the wires.

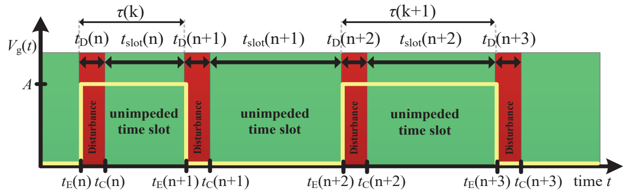

Fig. 3. General control signal (yellow), disturbance slot (red), unimpeded time slots (green) and used notation

A generalized ideal control signal can be described by a series of rectangular pulses with different pulse widths $\tau(k)$ and times of occurrence $t_{\mathrm{E}}(2k-1)$. The maximum amplitude A is constant and represents the logic level of the used signal. The general mathematical description of a control signal can be seen in (1).

$$V_{\mathrm{g}}(t) = \sum_{k=0}^{N_{\text{pulse}}} A \cdot \tau(k) \cdot \mathrm{rect}_{\tau(k)}\left(t - \frac{\tau(k)}{2} - t_{\mathrm{E}}(2k-1)\right) \quad (1)$$

The time slots $t_{\mathrm{slot}}(n)$ between the disturbing pulses allow an unimpeded communication. As control signal a pulse width modulation (PWM) is used in the following. For a PWM signal, the parameter $t_{\mathrm{E}}(2k-1)$ and $\tau(k)$ can be specified according to (2) and (3). The set point signal is defined as sine with A_{s} and f_s. The reference signal to generate the PWM signal can be a saw tooth signal with amplitude A_{PWM} and frequency f_{PWM}. The number of pulses N_{pulse} and therefore the switching edges depends on the considered periods of the set point signal N_{P} and the ratio of the used frequencies (4).

$$t_{\mathrm{E}}(2k-1) = \frac{1}{f_{\mathrm{PWM}}} \cdot k \quad (2)$$

$$\tau(k) = \frac{1}{2 \cdot f_{\mathrm{PWM}}} \cdot \left(1 - \frac{A_{\mathrm{s}}}{A_{\mathrm{PWM}}} \cdot \sin\left(2\pi \cdot f_s \cdot t_{\mathrm{E}}(2k-1)\right)\right) \quad (3)$$

$$N_{\text{pulse}} = \frac{f_{\mathrm{PWM}}}{f_{\mathrm{S}}} \cdot N_{\mathrm{p}} \quad (4)$$

In (1), ideal rectangular pulses are assumed which are adequately for the systematic investigations in this paper. If simulations on wire coupling should be done, a finite rise time is indispensable. The unimpeded time slots $t_{\mathrm{slot}}(n)$ between the disturbing pulses are specified according to Fig. 3. A vector $\vec{t}_{\mathrm{slots}}$ including all time slot durations in case of a PWM control signal can be calculated according to (5).

$$\vec{t}_{\mathrm{slots}} = \left[\vec{t}_k\right]_{k=0,..,N_{\text{pulse}}} \quad (5)$$

$$\begin{aligned}\vec{t}_k &= [t_{\mathrm{slot}}(2k-1),\ t_{\mathrm{slot}}(2k)]^{\mathrm{T}} \\ &= [\tau(k) - t_{\mathrm{D}}(2k-1),\ f_{\mathrm{PWM}}^{-1} - \tau(k) - t_{\mathrm{D}}(2k)]^{\mathrm{T}}\end{aligned}$$

In Fig. 4 the distributions of the values of $\vec{t}_{\text{slots}}$ considering one period of the reference sine ($f_{\text{s}} = 50$ Hz) are depicted for two different frequencies f_{PWM}. The amplitude ratio is determined with $A_{\text{S}}/A_{\text{PWM}} = 1$ for all presented investigations in this paper. In the left part of the figure, the histogram of the probability density is shown, whereas in the right part the cumulative distribution function can be seen.

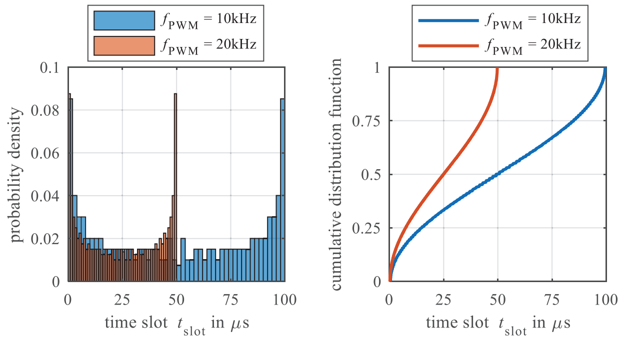

Fig. 4. Distribution of time slot duration for PWM signals with $f_{\text{s}} = 50$ Hz and $A_{\text{S}}/A_{\text{PWM}} = 1$ for $f_{\text{PWM}} = 10$ kHz and $f_{\text{PWM}} = 20$ kHz

III. Communication Methods For Disturbed Environments

In this section, the interfered transmissions are evaluated. The different operating strategies for the communication system are implemented in MATLAB and the resulting bitrates are calculated. The used configuration is defined in the previous chapter (cf. Fig. 2). The control signal is a PWM signal with different frequencies f_{PWM}. In CAN FD protocol payloads up to 64 Byte are specified. In Fig. 5 the maximum transmitted payloads depending on the available time slot are shown for three different bitrates. The frame length is not completely arbitrary because of the discrete values of payload length [1].

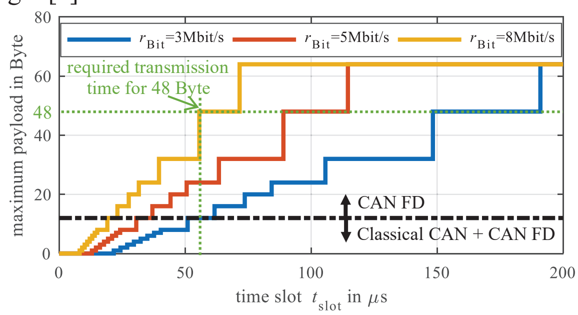

Fig. 5. Maximum transferable payload within available unimpeded slot

In the following investigations, a simplified CAN FD network is considered with a constant bitrate of 5 Mbit/s for the entire frame, i.e. there is no bitrate switching. The occurring disturbance slots are of equal length with duration of $t_{\text{D}}(n) = 1$ µs to make sure, that the disturbing pulse is decayed. The period of time under consideration is 0.5 s corresponding to 25 periods of the exemplarily chosen reference sine with $f_{\text{S}} = 50$ Hz to perform a statistical evaluation.

A. Event-triggered communication

The communication in classic CAN and CAN FD networks is event-triggered (ET) and uses CSMA/CA (Carrier Sense Multiple Access/Collision Avoidance) for medium access control [2]. In an ET system, transmissions are initiated whenever a node wants to transmit data to other nodes. Transmission conflicts are resolved by observing the message identifier. The node sending the object with the highest identifier will succeed. This access method is completely independent of the state of the power electronic system. An exemplary schedule of an ET communication on a recurring disturbed channel is depicted in Fig. 6. The start of a new frame is random as well as the frame length, based on the occurring events. In the figure it can be seen, that in this example only one frame is completely unaffected by the disturbing pulses.

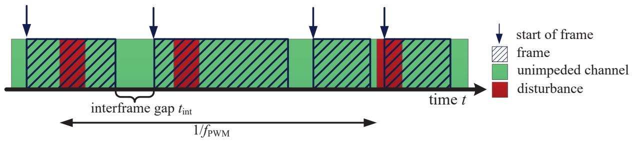

Fig. 6. Schedule of event-triggered communication

The net bitrate of the successful transferred frames within an event-triggered communication is determined now. A uniform distribution of frame length is chosen for the transmitted frames. The interframe gap is also uniformly distributed with a maximum value of 3 µs to emulate a high bus load. According to the specification, the entire frame is rejected, if a fault occurs during the transmission. The resulting net bitrate r_{t} includes all frames without any disturbance within their transmission time. The net bitrate depending on the frequency f_{PWM} is depicted in Fig. 7. It can be seen, that in all investigated configurations, the bitrate is significantly reduced compared to the ideal value of 5 Mbit/s. The average payload of the transferred frames is also shown in the figure. Because the frame length is uniformly distributed the ideal mean is 16.8 Byte represented by the dotted line. The unimpeded time slots are shortened by increasing PWM frequency and the probability for a long frame, fitting into an unimpeded time slot, drops. From a frequency of 13 kHz the transmission rate even decreases under the maximum bitrate of classical CAN (1 Mbit/s). In CAN FD protocol for event-triggered communication failed transmission attempts lead to resending of messages. The effective data transmission is thus even lower than the calculated bitrate. It could be concluded that communication can be seriously affected if communication and power electronics operate completely independent of each other.

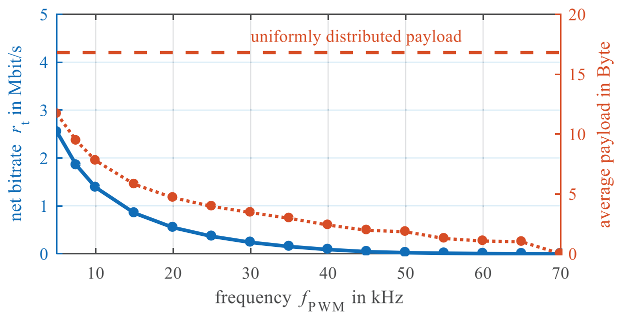

Fig. 7. Net bitrate of an event-triggered CAN FD communication and average payload of transmitted data

B. Time-triggered communication

To establish real time control and safety critical applications, time-triggered communication protocols were proposed [12]. In case of CAN, a higher-layer protocol was proposed to provide a time-triggered (TT) communication, which is specified in ISO11898-4 [2]. In TTCAN, a common time reference is introduced based on a network time unit (NTU). The cyclic transmission schedule is synchronized by the repeated transmission of a particular message, the reference message, which is transmitted by the time master. [13] The allocation of time slots for different nodes is based on TDMA (Time Division Multiple Access) and is statically defined within the development process. Every node gets a time slot within it can transmit its data. There is also the possibility of combined concepts of time- and event-triggered communication [14]. Within the basic cycle and the system matrix of a time-triggered communication, free time windows can be allocated. These windows can be used to avoid failed communication. A schedule, based on a time-triggered protocol, is shown in Fig. 8. In this method, the end of a disturbance is used as start of a new frame. The node gets a time slot to transmit its data. In this first method, the node tries to send all accrued data. As a consequence of this behavior, the frame could be too long to be transmitted in the available time slot or the time slot is not used efficiently. In the statistical evaluation, the frame length is chosen according to a uniform distribution.

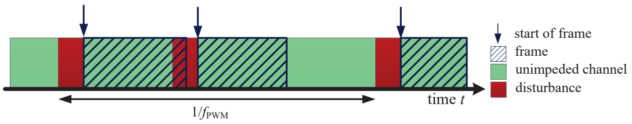

Fig. 8. Schedule of time-triggered communication with random selection of frame length

This time-triggered method is applied to the investigated setup. The calculated net bitrate and average payload are depicted in Fig. 9. The achieved net bitrates are higher and the average payload is equal in comparison to the event-triggered communication. It can be determined, that no communication is possible from a PWM frequency of 70 kHz, because the minimum frame length with payload of 1 Byte is too long to fit within the available time slots. Therefore no frame can be transmitted without an interference.

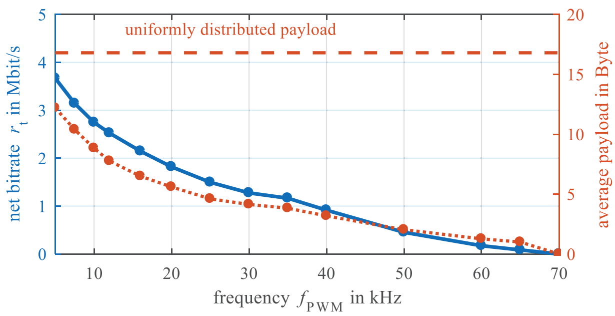

Fig. 9. Net bitrate of time-triggered CAN FD communication and average payload of transmitted data with random frame length

This time-triggered method is now optimized. The frame length is chosen according to the available unimpeded time slot. The schedule of this time-triggered method with adapted frame length is shown in Fig. 10. The sending node knows about the length of the available time slot and adjust the payload of its message. If there is further data to be transmitted, the next unimpeded time slot can be used to send the remaining data. If the residual duration of the time slot is long enough, another node may use this time to send its message.

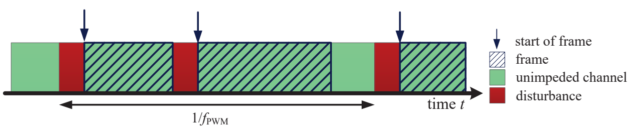

Fig. 10. Schedule of time-triggered communication with adapted frame length

The resulting net bitrate using this communication method is depicted in Fig. 11. It can be seen, that the net bitrate is higher in comparison to both previous presented communication strategies. The average payload used in the transmitted frames is also higher, because the maximum possible frame length is used and there is no random behavior restricting the efficiency. As in the previous investigations, the transmission rate decreases with increasing frequency. Despite this method there is no faultless transmission above a PWM frequency of 70 kHz. Therefore, no reliable communication can be established with a high transmission rate in a case of a high PWM frequency.

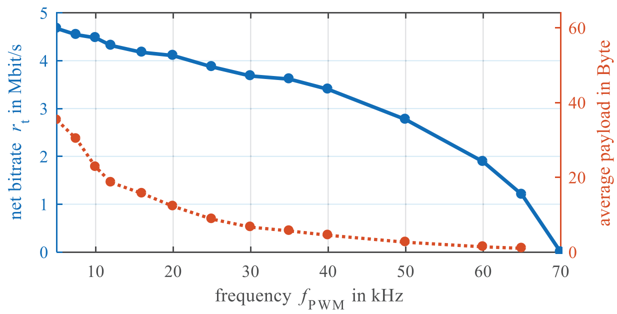

Fig. 11. Net bitrate of time-triggered CAN FD communication and average payload of transmitted data with adapted frame length

C. *Time-triggered communication with segmented frames*

The previous investigations point out the limits of communication within the described challenging electromagnetic environment. The unimpeded time slots have to be greater than the minimum frame length to ensure a transfer of an entire frame. This is the main problem of the previous presented methods, because above a frequency of 70 kHz, this condition is not met. In order to enable the increase of PWM frequency above 70 kHz and maintaining a reliable fast communication, a new operating method has to be introduced. The transmission of frames has to be interrupted during the occurrence of a disturbing pulse. After the disturbance is decayed, the transmission has to be continued. As a result, the transmission of one frame is split in several parts. The general schedule of this method is shown in Fig. 12. Two complete frames are shown and both have to be divided into two parts. This transmission affords the sending and receiving node to know about the times of disturbances. It also requires a global system time and the synchronization of all nodes within the network. This method is independent of the frame length and it can be adjusted to the send request. Therefore, the maximum payload can be used as often it is needed, which supports a high usable data rate.

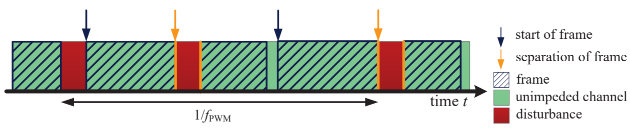

Fig. 12. Schedule of time-triggered communication with frame segmetation

The net bitrate rate r_t of this transmission method can be calculated with (6). The value of $t_{\mathrm{int}}(n)$ is nonzero, if there is an interframe gap within the regarded unimpeded slot n. In this calculation, the interframe gaps are reduced to zero to emulate a high busload. The net bitrate can be calculated as entirety of all bits, which could be transmitted in all available unimpeded time slots per one period of the set point signal.

$$r_{\mathrm{t}} = f_{\mathrm{s}} \cdot \left(\sum_{n=0}^{2 \cdot N_{\mathrm{pulse}}} \lfloor (t_{\mathrm{slot}}(n) - t_{\mathrm{int}}(n)) \cdot r_{\mathrm{Bit}} \rfloor \right) \tag{6}$$

In Fig. 13, the resulting net bitrate is depicted. The reduction of the bitrate is much lower than in the other presented methods, even for frequencies up to 100 kHz. With regard to the implementation, it could be useful to prohibit the segmentation of the header. The resulting net bitrates of this restriction are also presented in Fig. 13. In this case, the bitrate declines more steeply with increasing frequency. If the unimpeded time slots are shortened, the probability of an entire transmission of the header within the limited time of a single time slot diminishes and some time slots are not in use. Based on the segmentation the maximum frame length is not limited by the unimpeded time slots. This leads to a more efficient data transmission in comparison to the previously presented methods.

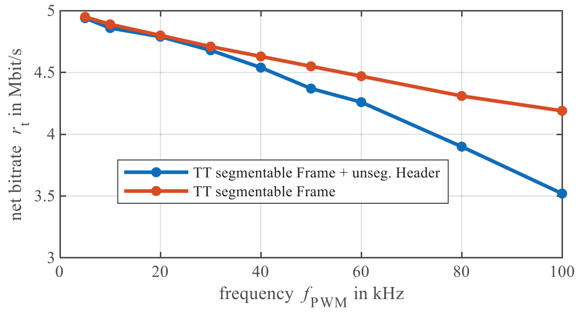

Fig. 13. Net bitrate of time-triggered CAN FD communication with segmentable frame

IV. Application

In the following chapter, the presented communication methods are deployed in a more complex setup compared to Fig. 2. In the next sections, the applicability and efficiency of the different communication methods are evaluated.

A. Setup

In this application example, a configuration with a DC/AC-converter based on WBG semiconductors and an asynchronous machine in a 48 V configuration is analyzed, as depicted in Fig. 14. Each half-bridge switches according to a pulse width modulation. To create the rotating field, the three PWM signals are phase-shifted with a difference of 120°. The three wires between the inverter and the electric machine can cause disturbing common mode pulses on a transmission line in proximity by wire coupling. As assumed, a transmission line of a point-to-point CAN FD network is very close to the three control wires within the wiring harness. The CAN FD communication is established with a transmission rate of 5 Mbit/s. Thus, the setup is similar to Fig. 2 but with 3 wires within the power electronic system generating the disturbance.

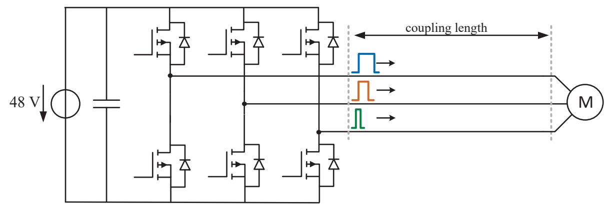

Fig. 14. DC/AC-converter as source of disturbance within a setup with cooperative operating method

In the left part of Fig. 15, extracts of the three PWM signals are shown. The signals are exemplarily determined for $f_{\mathrm{PWM}} = 20$ kHz. It can be seen, that the rising edges of all signals occur at the same time given by the PWM frequency. The falling edges are controlled by the modulation. The superposition of the three control signals shorten the duration of the unimpeded time slots between the edges in comparison to a single PWM signal. In the right part of Fig. 15, the cumulative distribution function of the available unimpeded time slots is presented. The minimum frame length is 13 µs (payload 1 Byte) and it can be seen that just 33 % of the unimpeded time slots are longer than this minimum value. In this configuration, the transmission without a segmentation of the frames would lead to a very low efficiency.

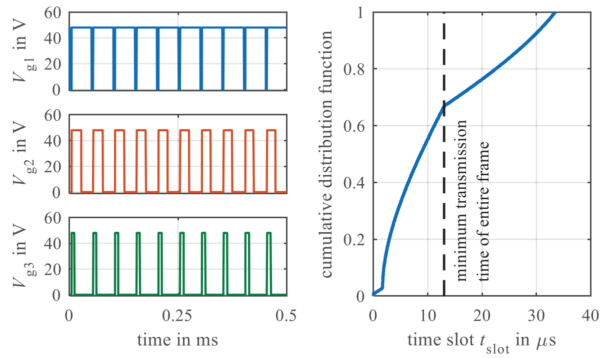

Fig. 15. Control signals of the inverter and cumulative distribution function of time slots ($f_{\mathrm{PWM}} = 20$kHz)

B. Analysis of net bitrates of different communication concepts

The resulting net bitrates of the different communication methods are shown in Fig. 16. It can be seen, that the three concepts transmitting entire frames lead to low net bitrates. Above a PWM frequency of 55 kHz no communication can be established by using these methods, because the maximum available unimpeded time slot is shorter than the minimum frame length. However, the time-triggered communication with adapted frame length leads to significantly higher net bitrates in comparison to event-triggered communication and time-triggered communication without adapting the frame length.

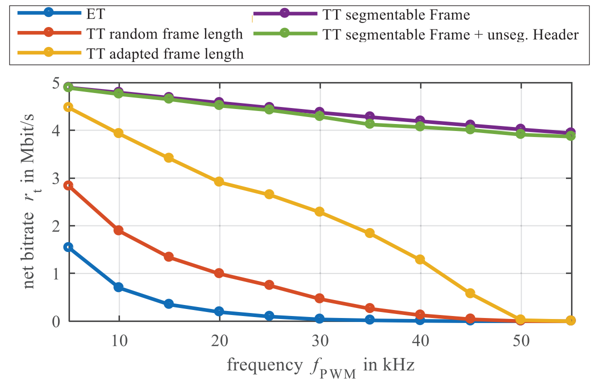

Fig. 16. Resulting net bitrate of different communication methods

The methods basing on frame segmentation provide good performances. The net bitrate is just reduced because of the rising number of impeded time slots with increasing frequency f_{PWM}. The difference between the resulting net bitrates of the two methods with segmentable frames is small. This corresponds to the results of chapter III.C. The raise of the bitrate r_{Bit} would lead to the same percentage deviation to the ideal value (c.f. (6)). Therefore, the presented communication method is appropriate for higher bitrates.

C. Analysis of latency of different communication concepts

In addition to the bitrate, the latency time t_L provides information about the performance of the communication. Within the event-triggered method and the time-triggered communication without adapting the frame length the frequent transmission failures of messages can lead to high delay times. In Fig. 17 (a) the mean latency of one frame within an event-triggered communication depending on the PWM frequency is depicted. The latency is very high in an event-triggered communication, because there is a high probability of simultaneous occurrence of data signal and disturbance. This probability increases with higher payloads p, which can also be seen in the figure. After a failed transmission, the node tries to resend its message after a random waiting period. In Fig. 17 (b) the same investigation is done for time-triggered communication without adapted frame length. Only if an occurring time slot is long enough to transmit the entire frame, the transmission succeeds. The previous requests with shorter time slots lead to failed transmission and a latency occurs. The time-triggered method leads to a lower latency than the event-triggered method.

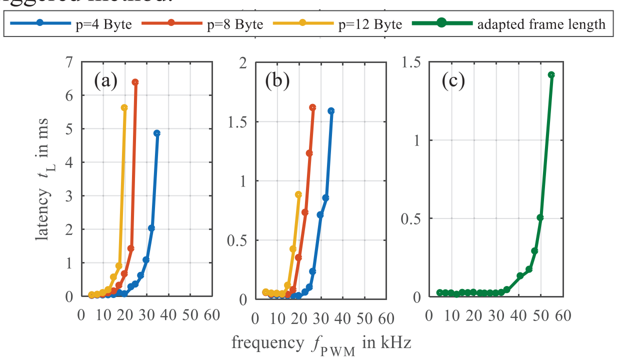

Fig. 17. Average latency of ET communication (a), TT communication with random selection of frame length (b) and TT communication with adapted frame length (c)

The time-triggered communication with adapted frames leads to no latencies until some available time slots are smaller than the minimum frame length (Fig. 17 (c)). With increasing number of unusable time slots, the delay rises significantly until all unimpeded time slots are too short to transmit an entire frame. Compared to this, the methods with segmented frames do not lead to any latencies because all slots are used to transmit parts of the message and the required transmission starts with the next available unimpeded time slot. However, the recurring paused transmissions lead to longer durations of transferred messages in comparison to a transmission on a complete unimpeded channel. This is quantified in the net bitrate presented in the previous section. The low performance loss within data rate is matched by high reliability in the transmission und a flexible applicability of the new presented approach.

V. Conclusion

A recurring disturbance caused by switching events of a power electronic system can lead to recurring common mode disturbances on wires nearby. In an event-triggered communication, there is a high probability of simultaneous occurrence of disturbing signal and data transmission. As a result, the effective transmission rate is greatly reduced.

In this work, the possibilities of time-triggered communication methods are discussed to reduce the impact of predictable disturbing signals. A new time-triggered communication method is proposed and analyzed in different simulative setups. This new time-triggered method uses the interruption of transmission within times of disturbance and segmented frames within the unimpeded time slots are transmitted. For this propose, a global time has to be introduced to enable all nodes to transmit and receive within the unimpeded time slots. The new method is analyzed in different setups and compared to common time-triggered protocols. The results show high reliability in configurations with frequently occurring disturbing pulses, even for communication systems with high transmission rates, this method is applicable. Therefore, the implementation of this method with other communication systems like Automotive Ethernet should be subject of further investigations.

Acknowledgment

The work in this paper was funded by the German Federal Ministry of Education and Research as part of the project RobKom (Robuste Kommunikation in autonomen Elektrofahrzeugen) with reference number 16EMO0380. The responsibility for this publication is held by the authors only.

References

[1] *CAN with Flexible Data-Rate Specification,* Version 1.0, Robert Bosch GmbH, 2011

[2] ISO-11898, Road Vehicles - Controller area network (CAN), International Standards Organization, 2015.

[3] CiA 610-1 version 0.0.0.4, CAN XL – Specifications and test plans – Part 1: Protocol and signal specification, CiA Special Interest Group (SIG), 2019 (available: https://www.can-cia.org/groups/technical-groups/technical-committee-tc/ig-layer-12/sig-can-xl)

[4] A. Lidow, *GaN Transistors for Efficient Power Conversion*, Chichester, Great Britain: Wiley, 2014

[5] K. S. Boutros, R. Chu and B. Hughes, “GaN Power Electronics for Automotive Applications,” IEEE Energytech, 2012

[6] H. Chen, T. Wang, “Estimation of Common-Mode Current Coupled to the Communication Cable in a Motor Drive System,” IEEE Trans. On electrom. comp., vol. 60, no. 6, 2018

[7] L. Ming and Z. Jingfeng, "Study on anti-jamming frequency selection in radar netting," *2016 2nd IEEE International Conference on Computer and Communications (ICCC)*, Chengdu, 2016, pp. 1781-1784

[8] S. T. Chung and A. J. Goldsmith, "Degrees of freedom in adaptive modulation: a unified view," in *IEEE Transactions on Communications*, vol. 49, no. 9, pp. 1561-1571, Sept. 2001

[9] S. Ö. Tengstrand, E. Axell, K. Fors, S. Linder and K. Wiklundh, "Efficient evaluation of communication system performance in complex interference situations," *2017 International Symposium on Electromagnetic Compatibility - EMC EUROPE*, Angers, 2017, pp. 1- 6.

[10] L. Xu, J. Li, M. Ouyang and J. F. Hua, "Integration of PEM fuel cell/battery powertrain: EMI noises and power split strategy," *Proceedings of 2011 International Conference on Electronic & Mechanical Engineering and Information Technology*, Harbin, 2011, pp. 787-792.

[11] *TLE9251V – High Speed Can FD Transceiver*, Rev. 1.1, infineon, 2018

[12] J. Rushby, “Bus architectures for safety-critical embedded systems”, *In Tom Henzinger and Christoph Kirsch, editors, EMSOFT 2001: Proceedings of the First Workshop on Embedded Software,* vol. 2211 *of Lectures Notes in Computer Science,* pp. 306-323, Lake Tahoe, CA, 2001

[13] F. Hartwich, B. Müller, et. al., “CAN Network with Time-triggered Communication”, Robert Bosch GmbH, 2001

[14] R. Obermaisser, “CAN emulation in time-triggered environment”, *International Symposium on Industrial Electronics (ISIE)*, vol. 1, 2002